Biophysical Chemistry 187–188 (2014) 23–28

Contents lists available at ScienceDirect

Biophysical Chemistry

journal homepage: http://www.elsevier.com/locate/biophyschem

# Force-dependent melting of supercoiled DNA at thermophilic temperatures

E.A. Galburt *, E.J. Tomko, W.T. Stump, A. Ruiz Manzano

*Department of Biochemistry and Molecular Biophysics, Washington University in Saint Louis, 660 South Euclid Avenue, Saint Louis, MO, 63110, USA*

## HIGHLIGHTS

- Temperature dependence of force-induced DNA melting on supercoiled templates.
- High-temperature single-molecule magnetic tweezers assay
- Thermophilic temperatures decrease critical tension at which DNA melts.
- Mesophilic and thermophilic strategies for DNA opening may differ.
- Estimation of *in vivo* DNA tension

## GRAPHICAL ABSTRACT

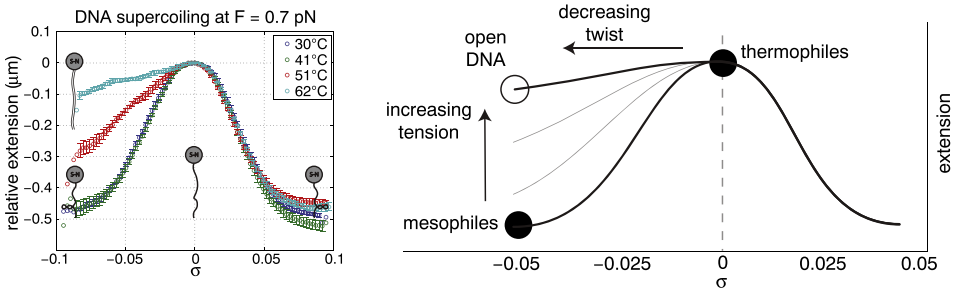


## ARTICLE INFO

*Article history:*
Received 5 December 2013
Received in revised form 7 January 2014
Accepted 7 January 2014
Available online 17 January 2014

*Keywords:*
DNA superhelicity
DNA melting
DNA tension
Single-molecule
Magnetic tweezers

## ABSTRACT

Local DNA opening plays an important role in DNA metabolism as the double-helix must be melted before the information contained within may be accessed. Cells finely tune the torsional state of their genomes to strike a balance between stability and accessibility. For example, while mesophilic life forms maintain negatively superhelical genomes, thermophilic life forms use unique mechanisms to maintain relaxed or even positively supercoiled genomes. Here, we use a single-molecule magnetic tweezers approach to quantify the force-dependent equilibrium between DNA melting and supercoiling at high temperatures populated by Thermophiles. We show that negatively supercoiled DNA denatures at 0.5 pN lower tension at thermophilic vs. mesophilic temperatures. This work demonstrates the ability to monitor DNA supercoiling at high temperature and opens the possibility to perform magnetic tweezers assays on thermophilic systems. The data allow for an estimation of the relative energies of base-pairing and DNA bending as a function of temperature and support speculation as to different general mechanisms of DNA opening in different environments. Lastly, our results imply that average *in vivo* DNA tensions range between 0.3 and 1.1 pN.



## 1. Introduction

DNA metabolism in all organisms is critically dependent on DNA melting. Replication, DNA repair, and transcription all require the opening of the DNA double-helix. However, single-stranded DNA is more susceptible to damage [1–3] and serves as an activator of the ATR-dependent DNA damage checkpoint [4]. Hence, a subtle balance between the double-stranded and open state of DNA must be maintained. This balance is dependent on environmental variables such as salt concentration, pH, torque, force, superhelical density ($\sigma = \Delta Lk/Lk_0$; i.e. the percent of extra or missing turns compared to B-form DNA), and temperature [5–8]. Interestingly, there are differences in superhelical density that correlate with differences in environmental temperature between Mesophiles (20 °C < T < 45 °C; $\sigma < 0$), Thermophiles (45 °C < T < 80 °C; $\sigma \approx 0$), and Hyperthermophiles (80 °C < T < 122 °C; $\sigma > 0$) [9–11]. In addition, hyperthermophilic Archaea have been shown to modulate their superhelical densities in response to either cold or heat shock [12]. These data suggest that DNA metabolism is viable only within a narrow range of

* Corresponding author.

0301-4622/$ – see front matter 
http://dx.doi.org/10.1016/j.bpc.2014.01.001

conditions where the DNA is poised between stability and denaturation. Here, to gain insight into these phenomena, we probe how temperature affects the force-dependent melting of negatively supercoiled DNA using single-molecule magnetic tweezers assays.

Single-molecule DNA manipulation is a powerful technique for probing the details of both the polymer physics of DNA itself as well as for directly observing the activity of enzymes that catalyze reactions on nucleic acids [13–15]. The magnetic tweezers are perfectly suited for studies of DNA melting and denaturation due to the ability to exert both force and torque on constrained DNA molecules [7,8,16–18]. The method depends on tethering DNA between a glass coverslip and a superparamagnetic bead. These linkages contain multiple individual bonds and generate a DNA "tether" that cannot relax torsionally. The beads are manipulated by changing the magnetic field gradient using permanent magnets mounted on a translatable and rotatable stage. The position of the bead is tracked in 3D and is used as a proxy for the position of the end of the DNA, thus allowing for measurements of the end-to-end distance of the DNA as a function of environmental conditions, enzymatic activity, protein binding, force, and torque.

Classic magnetic tweezers experiments showed that rotation–extension plots can be used to describe the relationship between DNA extension (end-to-end distance), force and superhelical density [16,17]. Rotation–extension plots have been used to study DNA buckling [19,20], the balance between supercoiling and DNA denaturation [7,8,16], and protein binding [21]. More specifically, after buckling, DNA responds to increased superhelical density by forming plectonemic writhes in a force-dependent and chiral manner (Fig. 1). Due to the conservation of linking number, extra turns (or links) introduced into the DNA by turning the magnetic bead must be absorbed by a combination of twist (Tw) or writhe (Wr); i.e. $\Delta Lk = \Delta Tw + \Delta Wr$. At low forces, positive and negative turns are absorbed by plectonemic writhes and the extension of the DNA decreases (Fig. 1a, lower curve) [16,17]. However, at higher forces, negative turns are absorbed by a reduction in twist, i.e. DNA melting (Fig. 1a, upper curve) [16,17]. This leads to a continuous reduction in the degree of compaction due to writhing as the force increases (Fig. 1b). The asymmetry is a direct result of the chirality of the double-helix and can be used as a sensitive measurement of DNA denaturation. Recently, this asymmetry has been used to study the details of the melting–writhing equilibrium [7] and its dependence on salt concentration and pH [8]. Here, for the first time, we extend these measurements to high temperature and determine the temperature-dependence of the characteristic force for the transition between writhing and denaturation at thermophilic temperatures.

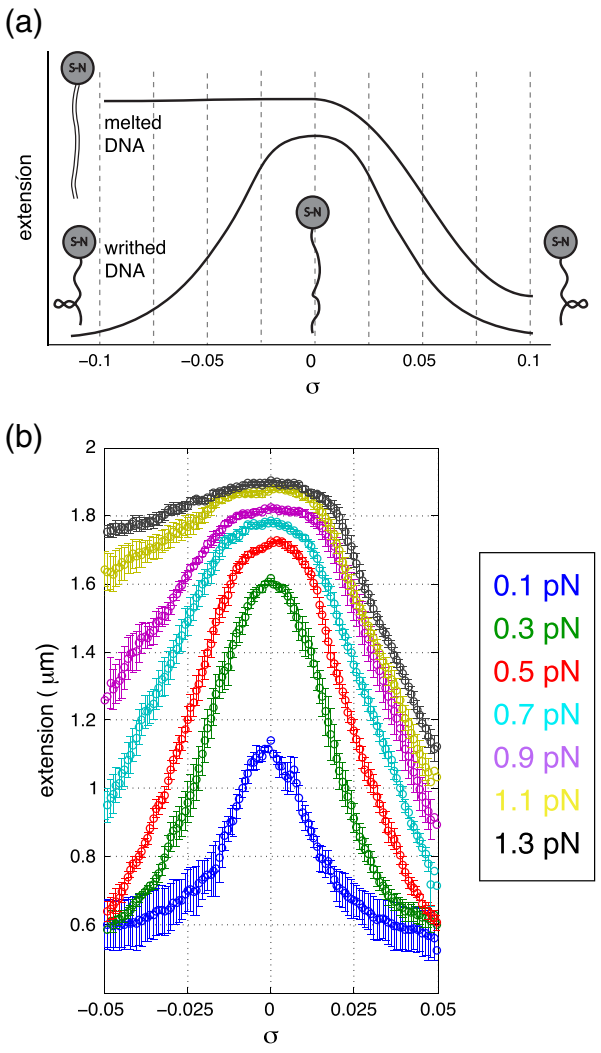


**Fig. 1.** (a) A schematic showing the force-dependence of DNA extension on superhelical density ($\sigma = \Delta Lk/Lk_0$). At low forces, extension varies symmetrically with increasing positive and negative turns. At high forces, the negative arm becomes flat due to DNA denaturation (melting). (b) Example of the force-dependence of rotation–extension curves for a 6 kb fragment of lambda DNA (bases 16759–22758).

## 2. Materials and methods

### 2.1. Flow cell construction

Drilled and un-drilled glass coverslips were sonicated in isopropanol for 15 min and then washed 3 times with water. They were coated with 3 μL of a 1 mg/mL nitrocellulose solution in amyl acetate and left to dry for 10 min. Cut parafilm spacers were sandwiched between a drilled and un-drilled coverslip and melted at 125 °C. After washing with PBS (10 mM NaPO4, 150 mM NaCl, pH 7.4), the cell was incubated with a solution of reference carboxylated polystyrene beads (1:1000 dilution in PBS, Spherotech, CP-15-10, 1.89 μm) for 5 min. After a PBS wash, the cell was incubated with anti-digoxigenin sheep antibodies (Roche, 0.1 mg/mL in PBS) at room temperature for 2 h. Lastly, the cells were passivated with a concentrated solution of BSA (New England Biolabs (NEB), B9001, 10 mg/mL) incubated at 4 °C overnight.

### 2.2. DNA tether and magnetic bead preparation

DNA tethers were constructed via published protocols [22]. Briefly, 1 kb biotin- and digoxigenin-labeled DNA handles were generated by PCR in the presence of labeled dUTP nucleotides (biotin-16-dUTP or digoxigenin-11-dUTP, Roche). A 2.2 kb core DNA template was also generated by PCR using a DNA template containing the SSVT6 promoter construct from *Methanococcus jannaschii* (gift of D. Grohmann, TU Braunschweig, supplemental information). These fragments were digested with MluI (NEB, R0198) and NheI (NEB, R0198) and ligated with a 4-fold molar excess of handles with T4 DNA ligase (NEB, M0202S). The final 4.2 kb product was gel purified to remove un-ligated DNA handles.

50 μL of streptavidin-coated magnetic beads (Dynabeads MyOne Streptavidin T1, Invitrogen, 1 μm, 65601) were passivated with three 1 mL washes of blocking buffer (PBS, 0.1% Pluronic acid F127, 1 mg/mL BSA) and resuspended in 50 μL of tweezing buffer (PBS, 0.1% Pluronic acid F127, 0.1 mg/mL BSA).

500 nL of 50 pM DNA template was mixed with 10 μL passivated beads and diluted immediately with 90 μL tweezing buffer. The DNA-bound beads were flowed into the flow cell and allowed to incubate for 10 min. Unbound beads were flowed out of the cell with 200 μL at 12 μL/min.

### 2.3. Magnetic tweezers

Data were acquired at 50 Hz on our magnetic tweezers apparatus that was built according to plans provided by the Seidel Lab (Biotech, Dresden, Germany) and published protocols [14,23,24]. Two cubic NdFeB magnets are mounted on a translatable and rotatable stage positioned over the flow cell holder of our home-built inverted microscope. The microscope is built around a 40× Zeiss objective lens (Plan NeoFluar, 440450) mounted on a piezo-electric focusing objective stage (PIFOC P-721, Physik Instrumente). A calibration curve of force vs. magnet height was constructed using the inverse pendulum model [17]:

$$F(z) = (k_B T \cdot L(z))/<\left(\Delta x^2(z)\right)>$$

where $F(z)$ is force at a magnet height $z$, $L$ is the end-to-end distance of the DNA at $z$, $\Delta x(z)$ is $x(z)$- $<x(z)>$, $k_B$ is the Boltzmann constant, and $T$ is temperature. Data taken at different magnet heights was used to fit the approximately exponential dependence $F(z) = Ae^{-Bz}$ [25].

### 2.4. Data acquisition and analysis

Lab-written LABVIEW software was used to implement both machine control and published bead tracking algorithms in 3D [14]. Briefly, a calibration image stack was created by imaging the beads out of focus over a range of bead-objective distances spanning 6 μm. This was done by moving the objective lens in jumps of 100 nm via the piezo-electric mount. The dependence of the resulting ring patterns on the distance of the bead from the objective was used to track the beads in the axial direction. Importantly, a correction factor due to the difference in index of refraction between the buffer and the glass/oil must be applied to the distances moved by the objective during calibration. Our empirical measurements using a published strategy resulted in a factor of 1.25 which agrees with the value for similar systems [26].

## 3. Results

### 3.1. Objective-based temperature control

Previous temperature-dependent single-molecule studies of DNA elasticity used techniques including indium tin oxide plates [27], copper water jackets [28], and high-conductivity copper plates [29] to heat the entire flow cell. Here, temperature control was implemented without any flow cell or microscope stage heating. Instead, an objective heater (Bioptechs, 150819-13) was used to heat the objective which then heated the flow cell sample locally via contact with the immersion oil. A calibrated thermocouple probe (Omega, 5TC-TT-T-40-36) was incorporated into a flow cell during parafilm melting and was used to measure the temperature as a function of distance away from the center of focus (Fig. 2). Measurements were taken for each of the temperature settings used in the experiments (30 °C, 40 °C, 50 °C, and 60 °C). With the thermocouple positioned directly over the objective, the measured values were 30 °C, 41 °C, 51 °C, and 62 °C respectively (±0.5 °C). Furthermore, the temperature was steady to within 1 °C within 1 mm away from the center of focus, suggesting that heat was efficiently transferred through the immersion oil to the objective-side coverslip and the buffer in the flow cell. In fact, as far out as 4 mm, the temperature at the 60 °C setting only drops to 55 °C showing that the DNA tethers being tracked are truly in a bath of the reported temperature. The method as reported is limited to 60 °C by the objective heater specifications and the desire to avoid damaging the objective lens. While higher temperatures may be possible, modification of the heater would be required and possible damage to the objective lens may occur.

Changes in temperature of the objective led to changes in the focus which were compensated by moving the flow cell in the lab frame (i.e. relative to the magnets). This change in focus was monitored using beads stuck to the flow cell surface as references. Over the full temperature range, an adjustment of 180 μm (~6 μm/°C) was required to keep the beads at the same focus. This change was highly reproducible suggesting that the objective lens was expanding and contracting without either hysteresis or damage. Magnet height was adjusted at each temperature to account for the change in flow cell position and to maintain a constant force. These adjustments corrected for very small errors in the force (i.e. $\Delta F \approx 0.05$ pN).

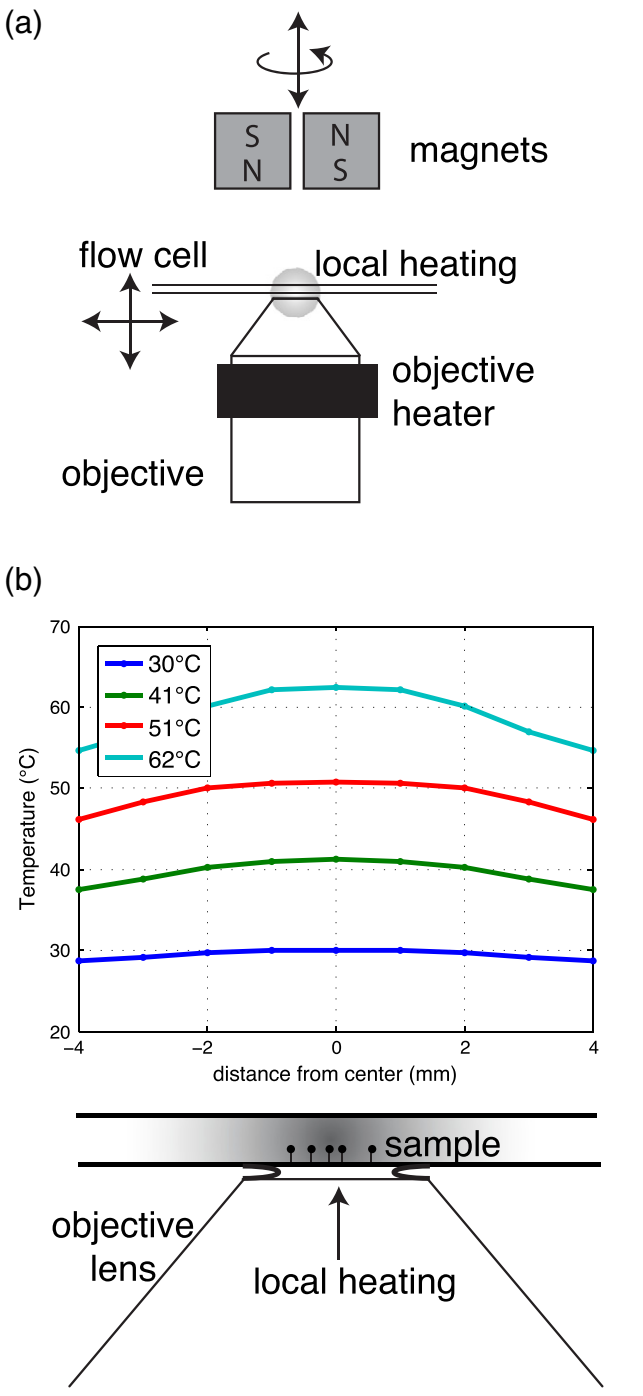


**Fig. 2.** Temperature control. (a) An inverted microscope is fitted with 2 NdFeB magnets on a rotatable and translatable stage. Local heating of the sample between 25 and 60 °C is accomplished using an objective heater as described in the text. (b) Empirical measurements of the temperature inside the flow cell indicate that heat is efficiently passed through the immersion oil to the sample.

### 3.2. Temperature-dependent denaturation-supercoiling transition

We collected rotation–extension curves at a range of forces and temperatures using 2.2 kb fragments of DNA containing the SSVT6 promoter construct from *M. jannaschii* (gift of D. Grohmann) and random handles. Using the objective lens heater-based approach (see above), data were collected at forces from 0.3 to 1.3 pN at four different temperatures (T = 30 °C, 41 °C, 51 °C, 62 °C). At each temperature, we observe the force-dependent transition from writhing to DNA denaturation as has been reported previously [16]. However, at higher temperatures the forces required to favor DNA denaturing are lower. The temperature trend can be seen when data taken at the same force are plotted together (Fig. 3). DNA held between 0.5 and 0.9 pN are the most sensitive to temperature. While we would expect extremely CG-rich or AT-rich sequence to change the propensity to melt versus writhe, similar results were obtained with 6 kb tethers taken from lambda DNA (bases 16759–22758; data not shown) suggesting that the trends shown here are not strongly dependent on either sequence or length.

To quantitate the temperature dependence, we measured the difference in extension between the −16 and +16 turns ($\Delta L_e$) as a function of force and temperature. This measure has been shown to accurately reflect the balance between DNA denaturation and supercoiling [7]. At 0.3 pN and 30 °C the DNA is compacted equally with negative and positive turns resulting in a $\Delta L_e$ equal to zero (Fig. 3a). As force and temperature increase, more DNA denaturation occurs, the negative arm becomes flatter, and $\Delta L_e$ increases. At 1.3 pN all the negative turns go into unwinding leading to a maximal $\Delta L_e$ of ≈0.4 μm (Figs. 3f and 4a). The characteristic midpoint of this transition (i.e. $\Delta L_e(F_{char}) \approx 0.2$ μm) occurs at ≈1 pN at 30 °C, while at 62 °C it decreases to ≈0.5 pN (Fig. 3b). Requiring that at 100 °C the DNA is completely melted in the absence of force ($F_{char} = 0$), the dependence of $F_{char}$ on temperature follows a sigmoidal curve with a midpoint temperature at 60 °C

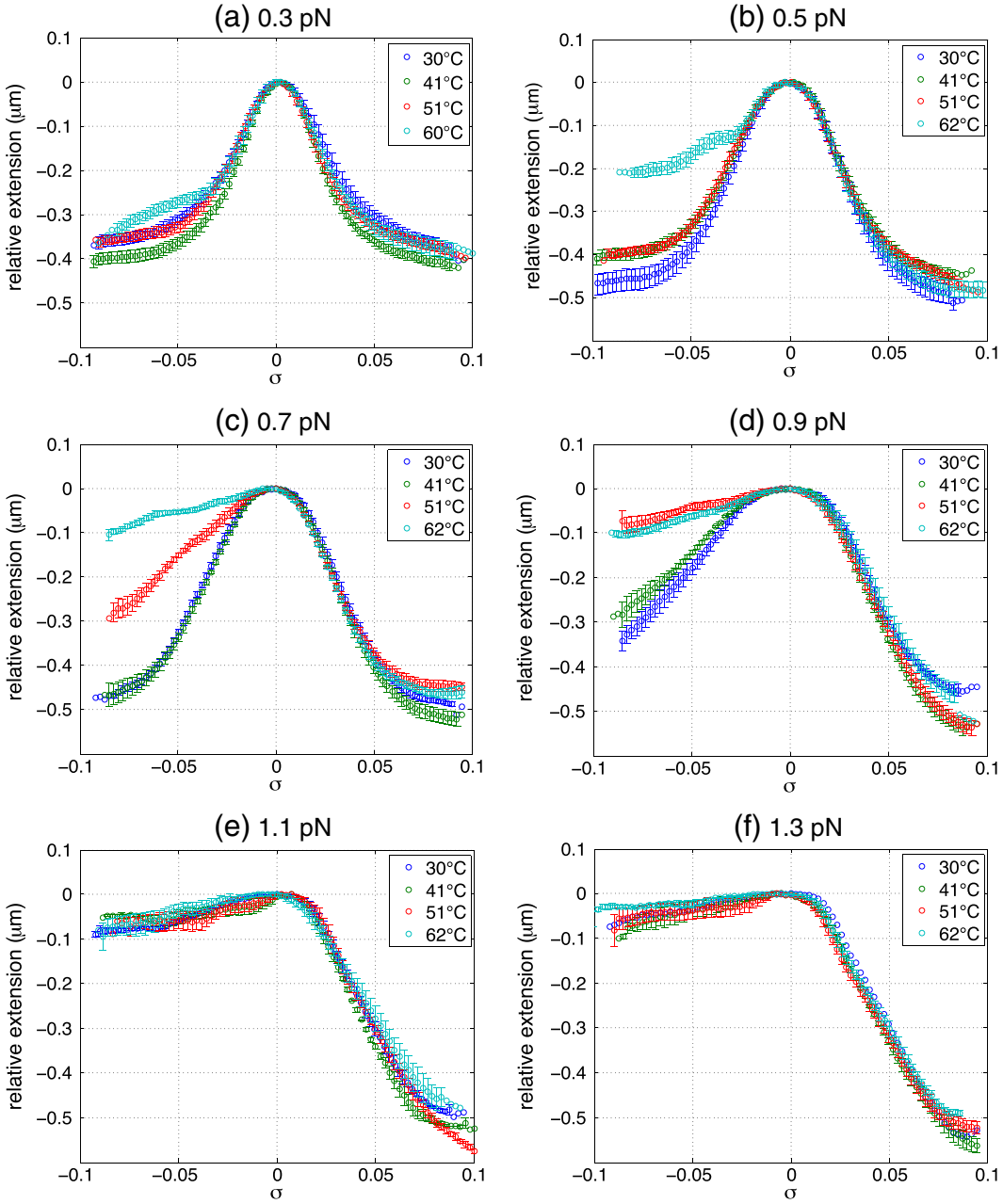


**Fig. 3.** Temperature-dependence of rotation–extension curves at (a) 0.3 pN, (b) 0.5 pN, (c) 0.7 pN, (d) 0.9 pN, (e)1.1 pN, and (f) 1.3 pN. Curves at different temperatures were collected on the same DNA molecules.

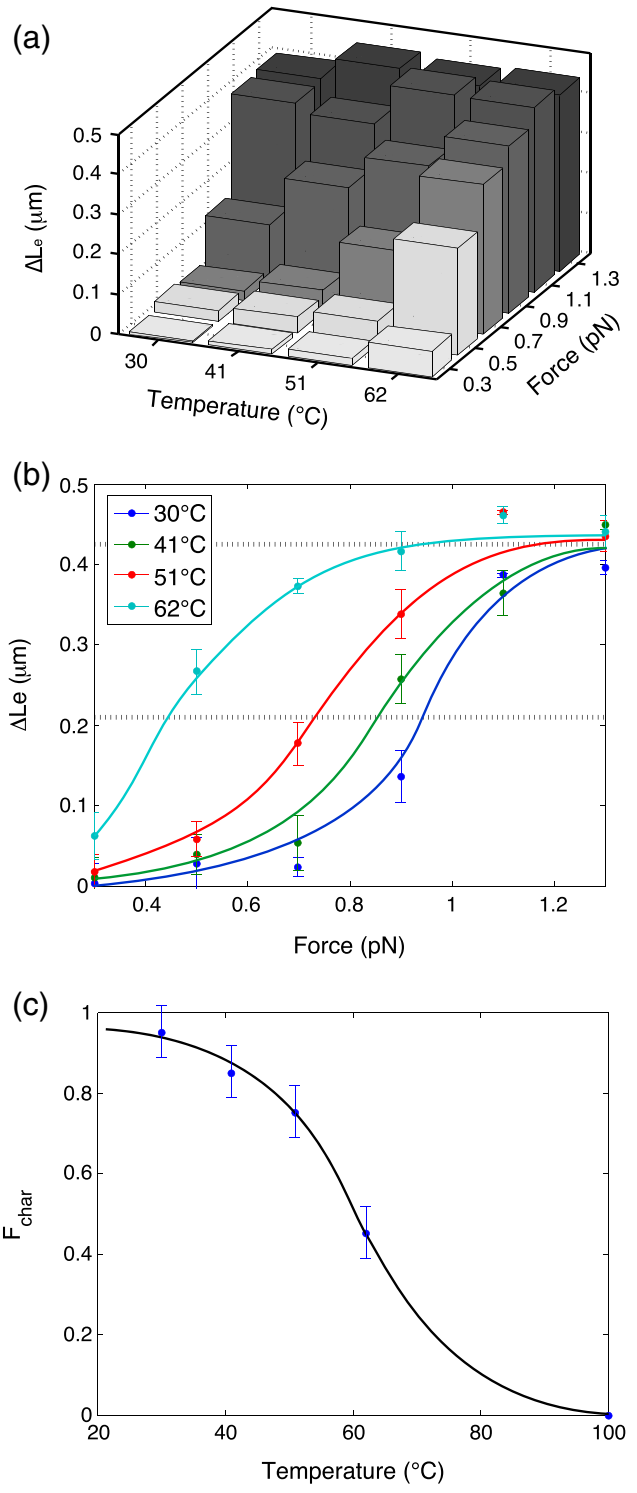


**Fig. 4.** Temperature- and force-dependence of DNA denaturation. (a) $\Delta L_e(F,T)$ is plotted for each force and temperature measured and varies from 0 to 0.4 μm. $\Delta L_e$ is calculated as the difference in extension between −16 and +16 turns. (b) $\Delta L_e$ vs. $F$ at different temperatures. (c) $F_{char}$ vs temperature (curve drawn through points as a guide to the eye).

(Fig. 4c). The amplitude of this curve (i.e. $F_{char}$ at low temperatures) is known to change as a function of salt concentration and pH [8]. Furthermore, we predict that the midpoint temperature will be lower under conditions favoring unwinding, such as low salt concentration or AT-rich sequence, consistent with a reduction in melting temperature under these conditions [5,6].

The characteristic force of this transition has been shown to be determined by the balance between energies of DNA denaturation and plectonemic writhing. The relationship between the force ($F_{char}$), the energy for denaturing a turn of base-pairs (α) and the bending energy of dsDNA (B) can be written as [7]:

$$F_{char} = \alpha^2 / \left(8\pi^2 B\right).$$

The persistence length of DNA ($L_p = B/k_BT$) has been shown to decrease by approximately a factor of two as a function of temperature across the range of our data [27,30]. Therefore, the two-fold reduction in $F_{char}$ from 30 °C to 62 °C would have to result from a two-fold decrease in base-pairing energy across the same temperature range.

These data describe the relationship between force and temperature as related to DNA denaturation. The observed temperature dependence of the negatively superhelical arm of the rotation–extension plots is consistent with the known temperature dependence of DNA melting. In contrast, no temperature-dependence was found on the positively supercoiled arm of the rotation–extension curve under the same conditions (Fig. 3, $\sigma > 0$). This is in line with the observation that an order of magnitude higher pulling forces is required to induce a change of state in positively supercoiled DNA [17].

These results lay the experimental ground work for magnetic tweezers experiments at high temperatures and allow for studies of the activity of thermophilic proteins with optimal activities at temperatures up to 60 °C.

### 3.3. Implications for general mechanisms of DNA opening

There is a strong correlation between environmental temperature and the superhelicity of genomes. All mesophiles have negatively supercoiled genomes and actively regulate superhelical densities to account for shifts in energy charge [31] and temperature [32]. However, Thermophiles and Hyper-thermophiles can been found with relaxed or even positively supercoiled genomes due to the exclusive presence of reverse gyrase in these organisms [33]. Furthermore, Thermophiles are also able to adjust linking number in response to heat- or cold-shock [12]. From these studies and others, it is clear that superhelicity is actively regulated to control DNA metabolism.

Assuming that the ground state of genomic DNA is closed and that small perturbations must lead to DNA opening to allow for DNA metabolism, our data can be used to speculate on general mechanisms of DNA denaturation in different biological environments. This assumption is likely fair as unwanted regions of open single-stranded DNA are generally harmful for cells [1–4] and yet, the genome must be routinely accessed by DNA/RNA polymerases and DNA repair enzymes. On our rotation–extension plots, we can place a moderately thermophilic organism with a relaxed genome at $\sigma = 0$ on the 62 °C curves (Fig. 5). At this temperature and superhelical density, the DNA satisfies our assumption as it is both stable (closed) and easily opened through small negative changes in superhelical density (Fig. 5, arrow to the left). This can be seen by looking at the 62 °C rotation–extension at 0.7 pN (Fig. 3c). On this curve, any decrease in superhelical density from relaxed DNA leads directly to denatured and accessible DNA. On the other hand, a mesophilic genome with a typical superhelical density of between −0.06 and −0.04 [10], will be placed $\sigma = -0.05$ on the 30 °C rotation–extension curves. Here again, the DNA is stable (closed), but may be easily opened by slight increases in tension (Figs. 3, 5, arrow up).

This line of reasoning suggests that energy from protein–DNA binding and ATP hydrolysis may be used in different ways in mesophilic and thermophilic organisms to locally denature DNA. In Thermophiles, energy would be used to locally reduce linking number, while in Mesophiles it would be used to locally increase tension. In both cases, the energy itself may be directly generated by proteins at their site of

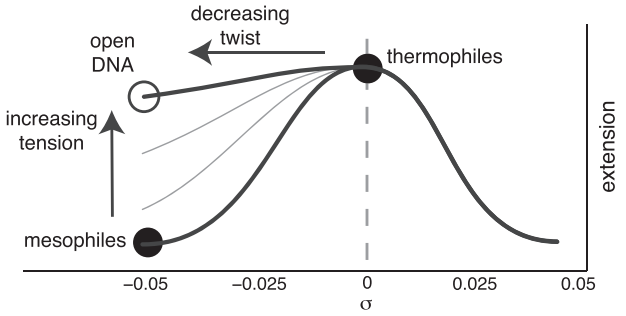


**Fig. 5.** Schematic diagram representing different strategies for producing a dsDNA genome that is both stable and accessible. The diagram assumes that the average DNA tension in the cell is between 0.3 and 1.1 pN (i.e. 0.7 pN; compare schematic to Fig. 3c). Mesophiles maintain a negatively supercoiled genome at 30 °C that allows small local increases in tension to lead to unwinding (arrow up). In contrast, Thermophiles maintain a relaxed genome at 62 °C that allows small decreases in $\sigma$ to lead directly to DNA unwinding (arrow to the left).

action via binding energy and ATP hydrolysis. However, indirect mechanisms where local DNA tension and or superhelicity are modulated by processes in DNA metabolism (i.e. transcription, replication, and topoisomerization) could also play a role.

The model predicts that DNA opening occurs along different degrees of freedom on the rotation–extension curve at different temperatures. These different paths are unique to each environment as increases in tension of these magnitudes (~1 pN) do not denature relaxed (or positively supercoiled DNA in the case of Hyper-thermophiles) and decreases in linking number do not denature negatively supercoiled DNA at mesophilic temperatures. Importantly, the particular degree of freedom (i.e. tension or superhelical density) that would control DNA opening in an organism would depend on the detailed environment of the nucleus. In addition to temperature and tension, environmental extremes in pH (acidophiles) or salt (halophiles), when not moderated by specific transport or metabolic pathways, would also have to be taken into account [8].

### 3.4. Average DNA tension in vivo

Assuming that average DNA tensions are of the same order of magnitude in Mesophiles and Thermophiles, the data combined with the models discussed above suggest that the average DNA tension *in vivo* lies somewhere in the range where our rotation–extension curves differ between 30 °C and 62 °C, namely between 0.3 and 1.1 pN. Only in this range of forces is the DNA perfectly balanced between stability of accessibility at both temperature ranges. These forces are reasonable as they are well within the working range of forces for proteins such as RNA polymerase [34], DNA polymerase [35], and Ftsk [36]. Furthermore, the high-sensitivity of DNA gyrase to tension, with an order of magnitude reduction in catalytic rate at 1 pN, is also consistent with sub-picoNewton DNA tension *in vivo* [37,38].

## Appendix A. Supplementary data

Supplementary data to this article can be found online at http://dx.doi.org/10.1016/j.bpc.2014.01.001.

## References

[1] K. Chan, J.F. Sterling, S.A. Roberts, A.S. Bhagwat, M.A. Resnick, D.A. Gordenin, Base damage within single-strand DNA underlies in vivo hypermutability induced by a ubiquitous environmental agent, PLoS Genet. 8 (2012) e1003149.
[2] S.A. Roberts, J. Sterling, C. Thompson, S. Harris, D. Mav, R. Shah, et al., Clustered mutations in yeast and in human cancers can arise from damaged long single-strand DNA regions, Mol. Cell 46 (2012) 424–435.
[3] T. Lindahl, Instability and decay of the primary structure of DNA, Nature 362 (1993) 709–715.
[4] K.A. Nyberg, R.J. Michelson, C.W. Putnam, T.A. Weinert, Toward maintaining the genome: DNA damage and replication checkpoints, Annu. Rev. Genet. 36 (2002) 617–656.
[5] P.L. Privalov, O.B. Ptitsyn, T.M. Birshtein, Determination of stability of the DNA double helix in an aqueous medium, Biopolymers 8 (1969) 559–571.
[6] D.Y. Lando, S.G. Haroutiunian, A.M. Kul'ba, E.B. Dalian, P. Orioli, S. Mangani, et al., Theoretical and experimental study of DNA helix-coil transition in acidic and alkaline medium, J. Biomol. Struct. Dyn. 12 (1994) 355–366.
[7] D. Salerno, A. Tempestini, I. Mai, D. Brogioli, R. Ziano, V. Cassina, et al., Single-molecule study of the DNA denaturation phase transition in the force-torsion space, Phys. Rev. Lett. 109 (2012) 118303.
[8] A. Tempestini, V. Cassina, D. Brogioli, R. Ziano, S. Erba, R. Giovannoni, et al., Magnetic tweezers measurements of the nanomechanical stability of DNA against denaturation at various conditions of pH and ionic strength, Nucleic Acids Res. 41 (2013) 2009–2019.
[9] P. López-García, DNA supercoiling and temperature adaptation: a clue to early diversification of life? J. Mol. Evol. 49 (1999) 439–452.
[10] F. Charbonnier, P. Forterre, Comparison of plasmid DNA topology among mesophilic and thermophilic eubacteria and archaebacteria, J. Bacteriol. 176 (1994) 1251–1259.
[11] F. Charbonnier, G. Erauso, T. Barbeyron, D. Prieur, P. Forterre, Evidence that a plasmid from a hyperthermophilic archaebacterium is relaxed at physiological temperatures, J. Bacteriol. 174 (1992) 6103–6108.
[12] P. Lopez-Garcia, P. Forterre, DNA topology in hyperthermophilic archaea: reference states and their variation with growth phase, growth temperature, and temperature stresses, Mol. Microbiol. 23 (1997) 1267–1279.
[13] C. Gosse, V. Croquette, Magnetic tweezers: micromanipulation and force measurement at the molecular level, Biophys. J. 82 (2002) 3314–3329.
[14] Y. Seol, K.C. Neuman, Magnetic tweezers for single-molecule manipulation, Methods Mol. Biol. 783 (2011) 265–293.
[15] I. De Vlaminck, C. Dekker, Recent advances in magnetic tweezers, Annu. Rev. Biophys. 41 (2012) 453–472.
[16] T.R. Strick, J.F. Allemand, D. Bensimon, A. Bensimon, V. Croquette, The elasticity of a single supercoiled DNA molecule, Science 271 (1996) 1835–1837.
[17] T.R. Strick, J.F. Allemand, D. Bensimon, V. Croquette, Behavior of supercoiled DNA, Biophys. J. 74 (1998) 2016–2028.
[18] T.R. Strick, V. Croquette, D. Bensimon, Homologous pairing in stretched supercoiled DNA, Proc. Natl. Acad. Sci. U. S. A. 95 (1998) 10579–10583.
[19] S. Forth, C. Deufel, M. Sheinin, B. Daniels, J. Sethna, M. Wang, Abrupt buckling transition observed during the plectoneme formation of individual DNA molecules, Phys. Rev. Lett. 100 (2008) 148301.
[20] H. Brutzer, N. Luzzietti, D. Klaue, R. Seidel, Energetics at the DNA supercoiling transition, Biophys. J. 98 (2010) 1267–1276.
[21] S. Zorman, H. Seitz, B. Sclavi, T.R. Strick, Topological characterization of the DnaA–oriC complex using single-molecule nanomanipuation, Nucleic Acids Res. 40 (2012) 7375–7383.
[22] A. Revyakin, R.H. Ebright, T.R. Strick, Single-molecule DNA nanomanipulation: improved resolution through use of shorter DNA fragments, Nat. Methods 2 (2005) 127–138.
[23] T. Strick, J. Allemand, V. Croquette, D. Bensimon, Twisting and stretching single DNA molecules, Prog. Biophys. Mol. Biol. 74 (2000) 115–140.
[24] T. Lionnet, J.-F. Allemand, A. Revyakin, T.R. Strick, O.A. Saleh, D. Bensimon, et al., Magnetic trap construction, Cold Spring Harb. Protoc. 2012 (2012) 133–138.
[25] J. Lipfert, X. Hao, N.H. Dekker, Quantitative modeling and optimization of magnetic tweezers, Biophys. J. 96 (2009) 5040–5049.
[26] M.T.J. van Loenhout, J.W.J. Kerssemakers, I. De Vlaminck, C. Dekker, Non-bias-limited tracking of spherical particles, enabling nanometer resolution at low magnification, Biophys. J. 102 (2012) 2362–2371.
[27] J.-S. Park, K.J. Lee, S.-C. Hong, J.-Y. Hyon, Temperature dependence of DNA elasticity and cisplatin activity studied with a temperature-controlled magnetic tweezers system, J. Korean Phys. Soc. 52 (2008) 1927–1931.
[28] H. Mao, J.R. Arias-Gonzalez, S.B. Smith, I. Tinoco, C. Bustamante, Temperature control methods in a laser tweezers system, Biophys. J. 89 (2005) 1308–1316.
[29] M.C. Williams, J.R. Wenner, I. Rouzina, V.A. Bloomfield, Entropy and heat capacity of DNA melting from temperature dependence of single molecule stretching, Biophys. J. 80 (2001) 1932–1939.
[30] S. Geggier, A. Kotlyar, A. Vologodskii, Temperature dependence of DNA persistence length, Nucleic Acids Res. 39 (2011) 1419–1426.
[31] G.W. Hatfield, C.J. Benham, DNA topology-mediated control of global gene expression in Escherichia coli, Annu. Rev. Genet. 36 (2002) 175–203.
[32] E. Goldstein, K. Drlica, Regulation of bacterial DNA supercoiling: plasmid linking numbers vary with growth temperature, Proc. Natl. Acad. Sci. U. S. A. 81 (1984) 4046–4050.
[33] C. Bouthier de la Tour, C. Portemer, M. Nadal, K.O. Stetter, P. Forterre, M. Duguet, Reverse gyrase, a hallmark of the hyperthermophilic archaebacteria, J. Bacteriol. 172 (1990) 6803–6808.
[34] M.D. Wang, M.J. Schnitzer, H. Yin, R. Landick, J. Gelles, S.M. Block, Force and velocity measured for single molecules of RNA polymerase, Science 282 (1998) 902–907.
[35] B. Ibarra, Y.R. Chemla, S. Plyasunov, S.B. Smith, J.M. Lázaro, M. Salas, et al., Proofreading dynamics of a processive DNA polymerase, EMBO J. 28 (2009) 2794–2802.
[36] P.J. Pease, O. Levy, G.J. Cost, J. Gore, J.L. Ptacin, D. Sherratt, et al., Sequence-directed DNA translocation by purified FtsK, Science 307 (2005) 586–590.
[37] J. Gore, Z. Bryant, M.D. Stone, M. Nöllmann, N.R. Cozzarelli, C. Bustamante, Mechanochemical analysis of DNA gyrase using rotor bead tracking, Nature 439 (2006) 100–104.
[38] M. Nöllmann, M.D. Stone, Z. Bryant, J. Gore, N.J. Crisona, S.-C. Hong, et al., Multiple modes of Escherichia coli DNA gyrase activity revealed by force and torque, Nat. Struct. Mol. Biol. 14 (2007) 264–271.